Journal of Advanced Research in Applied Sciences and Engineering Technology

Journal homepage:
https://semarakilmu.com.my/journals/index.php/applied_sciences_eng_tech/index
ISSN: 2462-1943

Growth Time Dependence on ZnO Nanorods Photoanode for Solar Cell Applications

Nurul Aliyah Zainal Abidin[1], Faiz Arith[1,*], Adri Aflah Shahrin Amri[1], Ahmad Nizamuddin Mustafa[2], Hafez Sarkawi[2], Mohd Shahadan Mohd Suan[3], Ahmad Syahiman Mohd Shah[4], Siti Aisah Junos[1], Fauziyah Salehuddin[1]

[1] Faculty of Electronic and Computer Engineering, Universiti Teknikal Malaysia Melaka, Hang Tuah Jaya 76100 Melaka, Malaysia
[2] Faculty of Electrical and Electronic Engineering Technology, Universiti Teknikal Malaysia Melaka, Hang Tuah Jaya 76100 Melaka, Malaysia
[3] Faculty of Manufacturing, Universiti Teknikal Malaysia Melaka, Hang Tuah Jaya 76100 Melaka, Malaysia
[4] Department of Electrical Engineering, College of Engineering, Universiti Malaysia Pahang, Lebuhraya Tun Razak, Gambang, Pahang, Kuantan, 26300, Malaysia

ARTICLE INFO

Article history:
Received 28 March 2023
Received in revised form 12 May 2023
Accepted 24 May 2023
Available online 1 August 2023

Keywords:

Zinc Oxide; Nanorods; Dye-sensitized solar cell; Photoanode; Hydrothermal

ABSTRACT

This work focuses on Zinc Oxide (ZnO) nanorods as the photoanode in Dye-Sensitized Solar Cell (DSSC). The photoanode protects the dye molecules and enables the energetic absorption of photogenerated electrons from the active state of the natural dye. The primary goals are the fabrication of ZnO nanorods on ITO, the investigation of the structural, optical and electrical properties of the synthesized ZnO nanorods, and the performance evaluation of the ZnO nanorods-based DSSC. The hydrothermal process is used to produce ZnO nanorods at an annealing temperature of 90°C. For structural characterization, a scanning electron microscope (SEM) with specific field ranges and magnification utilized to analyze and evaluate the composition of ZnO nanotubes. X-ray diffraction measurements with data processing are carried out in order to classify the crystalline process of the materials and provide information on cell unit size. Alternatively, UV analysis is used to demonstrate optical characteristics. Ruthenium was implemented as a natural dye, and four samples of ZnO nanorods with different development durations were tested for current density and voltage using an automated multimeter and UV irradiation. Calculations are performed for both current and voltage outputs of the DSSC.

1. Introduction

Solar energy, which the sun provides in the form of heat and radiation, is constantly released into the universe. Solar energy offers an unlimited, free source of clean, renewable energy. The ability to convert sunlight into solar energy using small and medium-sized photovoltaic (PV) cells is the main advantage of solar energy over other traditional generators. Affordable for ordinary people, solar energy has been plentiful in the last decade compared to fossil fuels and oil. In comparison, the labor

* *Corresponding author.*
E-mail address: faiz.arith@utem.edu.my (Faiz Arith)

https://doi.org/10.37934/araset.31.2.339351

costs associated with renewable energy sources are much lower than those of traditional electricity generation methods. Given various advantages, this capacity still has a few disadvantages. First, the sun's rays do not shine during the night. Second, sun exposure is not always present. To solve this problem, highly efficient solar cells and modules are required [1].

In recent years it has been shown that the current energy supply structure has no future. As a result, rising oil and gas prices are a blatant expression of the scarcity of these resources. At the same time, we are seeing the early consequences of fossil fuel use through melting ice, rising water levels, and poor weather conditions. Fortunately, renewable energy sources can be used to ensure a steady flow of electricity. They use infinite energy sources and can guarantee maximum supply through a mix of biomass, photovoltaics, water, etc. Photovoltaics make a significant contribution to the total amount of renewable energy. It enables the pollutant-free conversion of sunlight into electricity and would be an important part of future energy systems due to its enormous potential [2].

First-generation solar cells are built from silicon wafers. Its great power has made it the most widespread and oldest technology. Monocrystalline silicon solar cells and polycrystalline silicon solar cells are two subgroups of the technology category on silicon wafers. Second-generation solar cells are made of thin films and amorphous silicon (a-Si), less expensive than their predecessors made from silicon wafers. In comparison, light-absorbing layers in silicon wafer cells are often up to 350 m thick, but in thin-film solar cells, they are normally only 1 m thick. Thin film solar cells contain materials like copper indium diselenide (CIGS), amorphous silicon (A-Si) and cadmium telluride (CdTe) while the third generation solar cells consist of Nanocrystal solar cells, polymer-based solar cells, dye-sensitized solar cells (DSSC) and lumped solar cells [2]. In general, solar cells are constructed as PIN diodes, consisting of the hole-transporting layer (p-type) and the electron-transporting layer (n-type), both of which layers play a vital role in the efficiency of the solar cells. Commonly used electron transport layers are made of metal oxide materials such as ZnO [3] and TiO_2 [4] since both have almost the same bandgap energy and photocatalytic capacity. Meanwhile, CuSCN is the most commonly used hole transport layer as it is the best-performing material with significant conductivity [5-7].

1.1 Dye-sensitized Solar Cell (DSSC)

Thin-film solar cells DSSC due to their low cost, simplicity of production, and low toxicity, they have been studied for over 20 years. However, due to the high price, lower availability and lower long-term reliability, there is great potential for replacing established DSSC devices [8]. DSSC is an effective low-cost alternative to traditional solar cells [9-10]. A DSSC carries out three key measures to turn light from the sun into electric power: it depends mostly on obvious photo-excitation of the dye, which induces the electron transfer to the metal oxide semiconductor conductive band, accompanied by the recovery of electron donation from the redox torque in the electrolyte to the oxidised dye molecules, followed by electron mobility through the external load [11-12].

The entire process requires the assistance of various components of the DSSC, such as a light absorber through dye or sensitizer, an electron transfer agent and a hole transport agent [13,14]. In addition, in order for the DSSC to work, all of the components that make up the process will perform their tasks effectively. In general, sensitizer or dye may have particularly important properties for efficient efficiency, namely wide and heavy absorption from visible to near-infrared regions [15-17], chemical stability of the required LUMO and HOMO rates for effective injection of load into the semiconductor [18, 19] and electrolyte regeneration dye, high molar extinction coefficients for light harvesting in the visible and near-infrared region, nice solubility and photostability to hinder recombination [20, 21]. NS Noorasid et al. fabricated a complete DSSC by screen printing with TiO_2

as the photoanode in 2021. To investigate the effect of the annealing process, the deposited TiO_2 thin film was annealed at different temperatures. It was discovered that the porosity structure increased with the increasing temperature and the same concept applies to the distance between the TiO_2 particles [22].

By changing the TiO_2 thickness from 1 to 50,000 nm, the operating temperature, the doping concentration and the defect density, N.S. Noorasid et.al in 2021 analysed the performance of DSSC by SCAPS-1D simulation. The results indicate that each of these elements plays a crucial role in improving DSSC [23]. Those elements were also influenced in the next generation of Perovskite Solar Cell (PSC) [24].

Besides TiO_2 photoanode, ZnO has also emerged as a promising candidate as a photoanode in improving the charge carrier mechanism with lower processing temperature. Alias et al. successfully simulated DSSC using SCAPS-1D by applying different doping concentrations and the adjustment of certain critical layer parameters. Using 3 mol% ZnO:Al photoanode and 4 mol% ZnO:Ni photoanode, cell efficiencies of up to 3.96% and 3.9%, respectively, were obtained. This evidence shows that the additional dopant improves charge carrier conduction and increases the PCE in DSSC [25]. A similar trend was also demonstrated in other types of solar cells such as PSC [26, 27]. Low-temperature processing conditions are essential in the fabrication of flexible solar cells, which use plastic substrates, and can also reduce processing costs [28].

1.2 Working Principle of DSSC

Figure 1 shows the classic DSSC architecture. A thin layer of sensitized mesoporous metal oxide semiconductor with an inorganic or organic dye forms the basis of the device. This mesoporous layer is formed over a transparent electrode supported on an acceptable substrate. The photoanode assembly is the working electrode of the device. The unit counter electrode consists of a transparent conductive film mounted on a suitable substrate. By pervading the porous structure of the semiconductor, an electrolyte solution containing a redox mediator is trapped between the two electrodes, creating an electrical connection between them [29]. DSSC solar cells operate under fundamentally different principles than ordinary solar semiconductor cells do. The charge carriers and the absorption of the light are not the separating processes in semiconductor solar cells. These two functions are independent of the DSSC. The injection of light generated electrons into the conduction band separates the charge and these shaped promoters are transported to the collector [30]. Due to its large absorption unit, the solar cell can absorb a large amount of sunlight through the use of dyes.

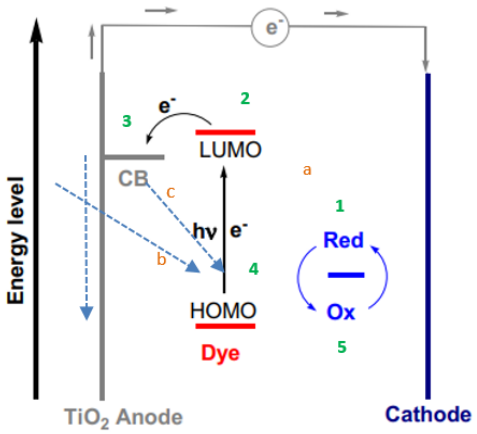

Fig. 1. Operation Principle of DSSC

1.3 DSSC using Zinc Oxide Nanorods (ZnO)

As a result of its excellent thermal performance, high thermal conductivity and high-temperature ZnO has many applications in industry. The properties of ZnO depend on the hexagonal close-packed wurtzite structure of Zn and O atoms [31]. ZnO processing techniques have been divided into metallurgical and chemical systems. It is classified in Category II-VI as a boundary covalence semiconductor between ionic and covalent semiconductors.

It is desirable for potential applications in optoelectronics, electronics, and laser technology due to its broad energy band (3.37 eV), outstanding structural efficiency (60 meV), and great thermal and mechanical stability at room temperature. These characteristics make it ideal for use in the future. The diversity of ZnO nanometric structures means that it can be identified as an emerging material for future applications in many nanotechnology fields [32]. A wide range of nanostructures including nanodots, nanotubes, nanotubes and nanonails, nanowalls, nanohelixes, seamless nanotubes, mesoporous single crystal nanowires and polyhedral cages have been developed [33].

ZnO nanotubes have been made by using thermal evaporation, metal-organic chemical vapour deposition (MOCVD), vapor-phase cycling, metal-organic vapour epitaxy, and thermal chemical vapour deposition. These growth methods are dynamic and call for high growth temperatures (more than 350℃). The hydrothermal solution has attracted a great deal of interest due to its particular advantages, which include its speed, low temperature (60℃-100℃), high yield and controllability compared to the above processes. Nishizawa *et al*., [34] produced needle-shaped ZnO crystals by hydrothermal synthesis (chemical deposition) by decomposition of an aqueous Na2Zn-EDTA solution at 330 °C [35].

Dye adsorption is a significant contributor to the conversion efficiency of ZnO nanorods array-based DSSCs, which are computed using the dye adsorption of individual nanorods arrays in conjunction with the number of nanorods arrays in a given area. A DSSC photoanode is a transparent TiO_2 membrane. ZnO, though, is seen as the most appealing option. For the first time in 2005, Baxter and Aydil developed ZnO nanorods based DSSC and obtained 0.5% of photo conversion efficiency (PCE) through hydrothermal technique [36]. Therefore, over the years, a large number of useful techniques have been utilized to synthesize nanorods. However, the hydrothermal technique has been shown to work particularly well for ZnO as it is a simple process, performed at a low temperature and at an affordable price. It produces a crystal clear structure with great shape and clarity, and is also a fast and regulated approach [37].

1.4 ZnO Nanorods Growth on Indium Doped Tin Oxide (ITO) substrate

On glass substrates, ZnO nanotubes were generated from ZnO film that was deposited by reducing the annealing process. DC sputtering was used to deposit thin films of varied thicknesses from 200 to 500 nm on top of the glass substrates. It shows that the thickness of the ITO films has a significant impact on both the structural and electrical properties of the ITO films [38]. Photo-spectrometer and Raman spectroscopy are the instruments that are used in the course of optical analysis. The roughness of ITO films increases as a direct consequence of their increased thickness. The versatility of the ITO films used in the Hall was also increased by increasing the film thickness, which reduced the resistance as a result of this.

ITO film with a thickness of 500 nm was found to produce the best mobility, which was 29.2 cm^2/V s, and the lowest resistance was 1.303×10^{-4} Ω-cm. The thickness of the ITO coating exerted a significant amount of impact on the structural characteristics of the ZnO nanotubes. Because of the increased thickness of the ITO sheet, the density of the ZnO nanotubes gradually lessened. The

growth mechanism and impact of the thickness of ITO films on the structural properties of ZnO nanotubes have been studied. ZnO nanotubes have been added to a DSSC as photoanodes. This color-sensitized solar cell conversion performance was 2.11% [38]. In general, the output of dye solar cells is assessed using a variety of cell parameters such as power conversion efficiency, fill factor, open circuit voltage, short circuit current, maximum voltage and maximum cell current [39].

2. Methodology

The production of DSSC required a number of different procedures and equipment in order to complete the process. The preparation of the substrates, the preparation for the development of the ZnO nanorods, the selection of an appropriate natural dye, the preparation of the electrolyte, and the determination of the counter electrode are the general techniques and procedures that are utilised in the fully fabricated DSSCs. In the manufacture of a ZnO nanorods solar cell, the procedures and mechanisms that have been discussed are normally the primary processes that are utilised.

2.1 Substrates preparation

The resistivity of the substrates was measured as the first step in this process. The resistance value is shown on the conducting side of the ITO, but there is no resistance value on the non-conductive side of the glass. This was done to ensure that the cutting line was drawn on the glass side. Because its effectiveness influences the results, the ITO side must be thoroughly maintained, free of scratches, and always clean. After measuring the resistance, the glass must be labelled to differentiate the varying periods required by four samples for the formation of ZnO nanorods. The substrates were then cleaned chemically using ethanol and acetone. To remove the light resistance, the substrates were individually soaked in acetone. It has no effect on microstructure, roughening, or oxide reduction. As a result, it is an efficient cleaning approach. This cleaning procedure just affects the surface and has no effect on the chemical or electrical qualities. The substrates were then immersed in the ethanol beaker. The ethanol level should be higher than the substrate level. As a result, the substrates can be fully immersed. With no overlap, all substrates were neatly put in the beaker. After that, the beakers were cleaned in an ultrasonic bath. The top of the beaker is covered with aluminium foil. For 10 min, the temperature was set to 70 °C. The substrates were placed on the hotplate with tweezers after the chemical cleaning process. The substrates were then dried for 5 min on a hot plate set to 90 °C. To ensure cleanliness, the clean substrates were positioned in a petri dish wrapped with aluminium foil after drying.

2.2 Seeding process

The production of ZnO nanorods is not similar to the production of TiO_2. It includes a set of chemicals and materials used to grow nanorods. ZnO nanorods are generally grown on ZnO seed layers using a hydrothermal method. Before growth, the ZnO seed layers are grown on a cleaned ITO. Thus, the first step in this process was to prepare a seed solution to form an ITO-based seed layer. The unit moles (M) for 1 mM zinc acetate dihydrate and 1 mM sodium hydroxide need to be converted to grams as this is easier to implement. Three beakers of the same size were used to mix different chemical solutions. The first beaker labeled A consists of 60 ml of ethanol mixed with 1 mM zinc acetate dihydrate [$Zn(O_2CCH_3)_2 \bullet 2H_2O$] the second beaker labeled B consists of 60 ml of ethanol mixed with 1 mM sodium hydroxide (NaOH) and the third beaker labeled C Beaker consists of 60 ml ethanol. The chemical solutions in beakers A and B were then stirred at 60 °C for 30 min at a speed

of 300 rpm. After stirring and heating, Beaker A and Beaker B were set aside to cool. The chemical solution in Beaker A (A+C) was then poured into Beaker C to mix Beaker A and Beaker C. As a result, the volume of the solution is 120 ml. By dropping 2 ml every 1 minute, the chemical solution in beaker B was synthesised into the chemical solution in beakers (A+C). At the same time, the chemical solution was stirred at a speed of 300 rpm and heated to 60 °C. The dropping operation of the chemical solution in beaker B was continuously performed until the solution was completely finished. The mixed solutions were subjected to double boiling at 60°C for 3 hrs using a magnetic stirrer. The timer was set manually.

After 3 hrs, the labeled ITO jars were immersed in the inoculation solution for 15 min. Then anneal it on a hot plate at 150 °C also for 15 min. Repeat 3 times. Next, dipped it back in and annealed it until dry. This time just dipped and tempered until dry, then dipped again without timing as before. Repeat it 10 times. After that, anneal the ITO for about 1 hr. The total of dipped and dry methods took 3 hrs including annealing. The aim of this process is to remove water and improve the electrical contact between the substrate and the ZnO seed layer. The resulting ZnO seed particles served as a nucleation center for the growth of nanotubes on ITO glass.

2.3 Growth process

The ZnO nanorods growth process was followed by a reaction of 10 mM zinc nitrate hexahydrate [$Zn(NO_3)2.6H_2O$] and 10 mM hexamethylene teramine or HMT [$(CH_2)6N_4$] dissolved in deionized (DI) water. As a seeding process, chemical materials also need to be converted to grams for the growth process. The molar unit (M) for 10 mM zinc nitrate hexahydrate and 10 mM HMT was calculated. ZnO growth solution was prepared by the resolution 4.4624 g of zinc nitrate hexahydrate and 2.1029 g of hexamethylene teramine or HMT in 750 ml of DI water to form a 10 mM aqueous solution. Four beakers were set up and each beaker consists of an inoculated ITO glass for growth. 8 rectangular pieces of glass were used to serve as the base for the growth solution flow at the bottom of the ITO page. Next, 250 ml of zinc nitrate hexahydrate or HMT was mixed in the beaker. Both solutions must be mixed in the oven about 5 min before coating, otherwise the chemical material will degrade if mixed for a long time. Then 100 ml of the mixed solution was poured into 4 beakers. Then the annealing process was carried out in the oven at 90 °C. The growth solution had to be changed every 5 hrs to avoid degradation. The manipulated variable is growth time and at 2 hrs the first sample was removed from the oven, at 2 hrs followed by 3 hrs, 5 hrs and 7 hrs. The growth conditions vary and are optimized since these parameters are crucial for the vertical alignment of the ZnO nanorods. The beaker becomes cloudy and white particles are distributed on the ITO surface.

2.4 Electrolyte and counter electrode preparation

The redox shuttle and electrolyte are made by combining 127 mg of iodine crystal, 830 mg of potassium iodide, and 10 ml of ethylene glycol. Both substances are properly combined in an opaque box to limit light absorption until totally dissolved. These concentrations were chosen to limit the recombination current and light absorption by tri-iodine ions, which causes decomposition. Another ITO glass is utilised to make the counter-electrode (cathode). The conductive side of the ITO glass is employed as a counter electrode. This results in a counter electrode that must be catalysed by the redox shuttle. However, the ITO must be cleaned using an ultrasonic bath to ensure its purity.

2.5 Final assembly

Glasses with ITO coatings are labelled A1 to A4. Upon completion of the sealing process, the coated samples are poured a few drops of dye solution. The ZnO nanorods layer receives electrons from the dye, which are then injected into the layer. A few drops of electrolyte are added to the sample and the slide is placed over it after 30 min. The samples must be oriented so that the coated surfaces are touching. Each slide has a conductive side that can be accessed in order to properly offset them. The edges become dots for both the negative and positive electrodes. The foil with the ZnO nanorods is the negative side, and the foil with the cap is the positive side. Prior to the sealant drying, the cell is held together by two clips. Alligator clips on a multimeter are used to make contact with the bare areas for a true reading of electrical conductance.

3. Results

3.1 Structural Properties (SEM and XRD)

The surface morphology of ZnO nanorods can be determined using Scanning Electron Microscopy (SEM). Observation and analysis under SEM were carried out on four samples with different growth times of ZnO nanorods. From Figure 2, the length of the ZnO nanorods was measured at random and reveals that sample A2 has a longer length compared to other samples, with 3 hrs of growth time. 5 hrs sample growth time is denser than other samples. The pore size (space between ZnO nanorods) increased as the growth time increased. This can be proven by the A1, A2 and A3 samples shown in Figure 2. However, the pore size started to decrease after 5 hrs of growth time. Thus, the morphology of A2 sample surface composition is better than other samples. This illustrates that it is necessary to conduct nanorods development for 3 hrs.

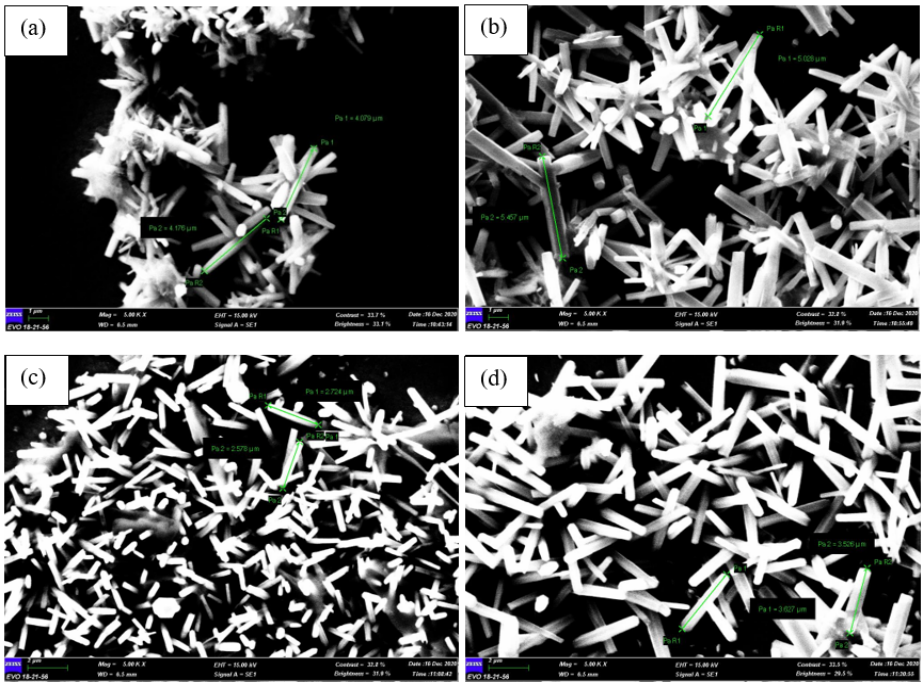

Fig. 2. SEM images of ZnO nanorods with different growth time (a)2hrs (b)3 hrs (c)5 hrs (d)7 hrs

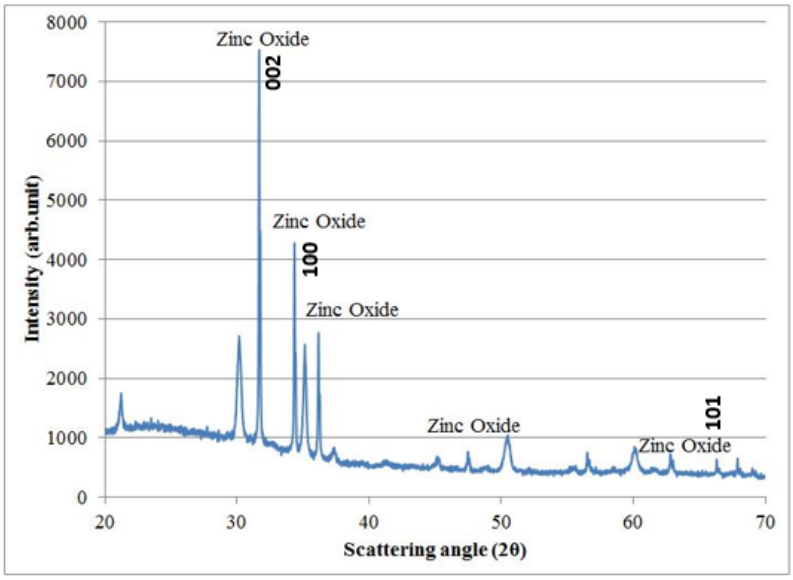

Fig. 3. XRD pattern for ZnO nanorods DSSC samples

Figure 3 is the XRD pattern graph for ZnO nanorods DSSC samples. The presence of zinc oxide proves that the ITO substrate is coated with zinc oxide. XRD is performed before the deposition of dye, electrolyte and counter electrode is made on the ITO substrate. The structure of all ZnO nanorods peaks is observed as zinc oxide hexagonal wurtzite. The XRD pattern shows that the ZnO nanorods crystal has an excellent level of uniformity, as evidenced by the sharp peaks in the pattern. The result obtained shows that the ZnO nanorods samples prepared by hydrothermal methods have a strong peak between 31.45° and 31.93° (2θ) corresponding to the (002) plane and have a pure hexagonal wurtzite structure with a high c-axis orientation. The second apparent peak (2θ) is between 34.12° and 34.52° and corresponds to the (100) plane based on the figure above, while the lowest peak shows that zinc oxide corresponds to the (101) plane at (2θ) coincides between 66.06° and 68.14°. The zinc oxide peaks in the XRD pattern prove that the seeding and growth process using ZnA, NaOH, ZnH and HMT to grow the ZnO on the ITO is successful.

3.2 Optical Properties (UV-VIS)

UV-Vis is used to determine the absorbance of samples A1, A2, A3 and A4 by applying a specific wavelength or lambda. In this project, wavelengths between 200 and 1000 nm were used. This is because the wavelength range of ultraviolet light is around 200 to 400 nm while the wavelength range of visible light is around 400nm to 800 nm. As shown in Figure 4a), the effect of the first UV-Vis layer was observed for ZnO nanorods DSSC. This chart contains four samples labeled A1, A2, A3, and A4. UV-Vis is used to measure the absorption property of ZnO. The sample with the highest absorbance is A3, followed by A2, A4 and finally A1. Analysis of the peak wavelength for each sample gives the identical value of 339.5 nm. Thus, it is confirmed that each sample has a ZnO coating and no other photoanode. In other studies, the peak wavelength for ZnO is between 300nm and 400 nm, which is proportional to the amount of energy required to shuttle the electron between energy levels.

A band gap is defined as the difference between the valence band and the conduction band of electrons. The band gap is the minimum amount of energy required to excite an electron in the conduction band into a conductive state. Figure 4b) illustrates the effect of the band gap for samples

A1, A2, A3 and A4, using UV-Vis spectroscopy. In order to calculate the band gap, Tauc plots is used. The chart is generated considering the average nanorods thickness, absorbance, absorptivity alpha, photon energy, and wavelength. All of the resulting samples have a band gap of about 3.3 eV. This shows that all samples have approximately the same band gap with ZnO, which is theoretically 3.37 eV. The Knee approximation method is used to determine the band gap of ZnO from its plot. This is the most common and simplest method used by other researchers to determine bandgap via graph. In addition, a goodness of fit (R^2) of 0.97815 was achieved, designating excellent accuracy.

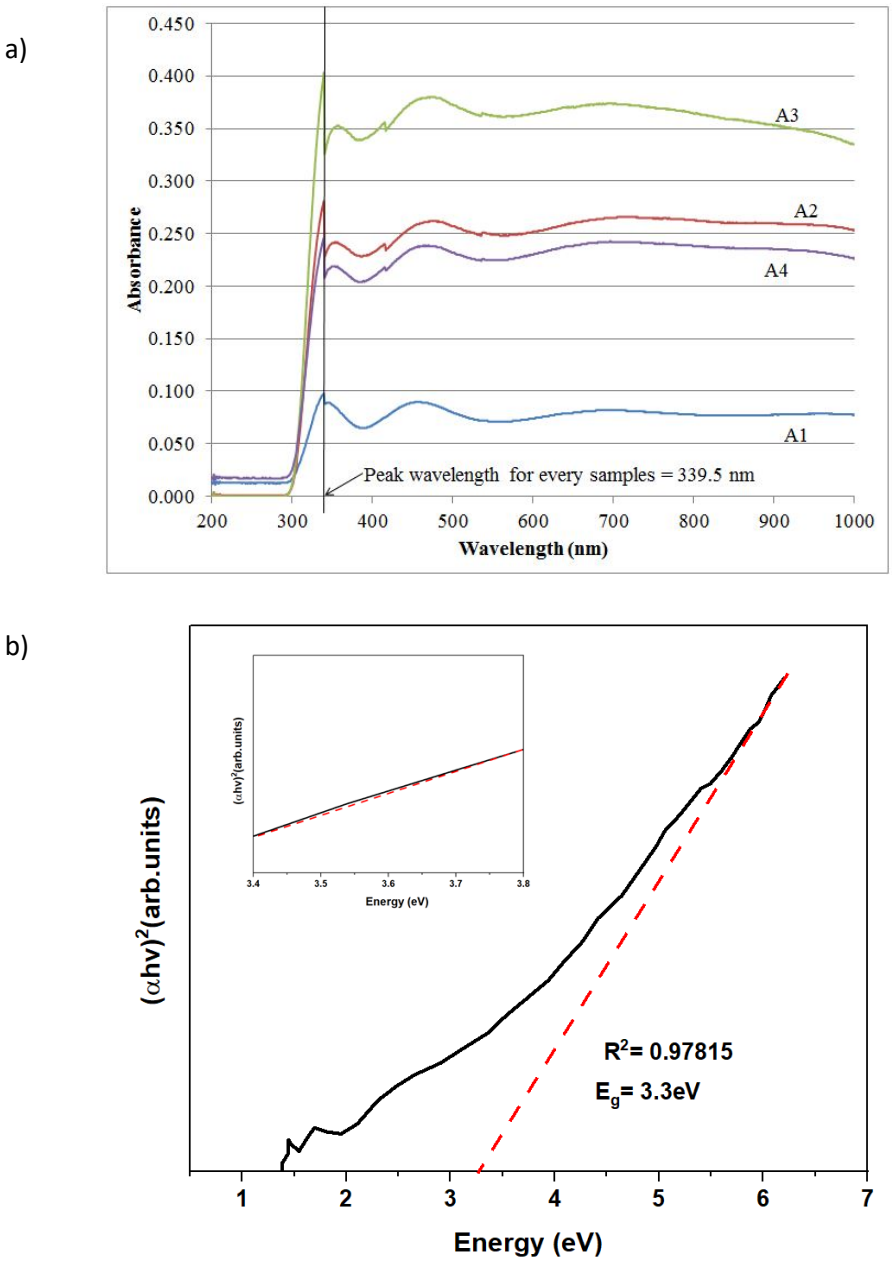

Fig. 4. a) UV-Vis first layer graph for ZnO nanorods DSSC b) Band gap effect on ZnO nanorods DSSC samples [inset, goodness of fit R^2 (plot)]

3.3 Electrical Properties (I-V Characteristics)

The measured voltage and current electrical properties of ZnO nanorods DSSC under solar UV irradiation are summarized in table 1. The voltage is supplied by the power supply, while the current is measured using Keithley 2401. The voltage applied is in a range of 2 V to 6 V. The result shows that sample A4 has the highest measured current compared to other samples. With increasing duration of the growth process, the measured currents also increase. Thus, by applying a voltage to ZnO nanorods DSSC, the conductivity and resistivity can be measured using the I-V characteristics. The best-measured voltage and measured current are A4 which resulting 0.741 V and 2.2 µA where the area of each sample exposed to the light is 3 cm^2.

Table 1
Electrical properties of measured voltage and measured current of ZnO nanorods DSSC

Sample	Growth Time of ZnO Nanorods (hrs)	Measured Voltage (V)	Measured Current (µA)
A1	2	0.317	1.1
A2	3	0.558	1.4
A3	5	0.645	1.7
A4	7	0.741	2.2

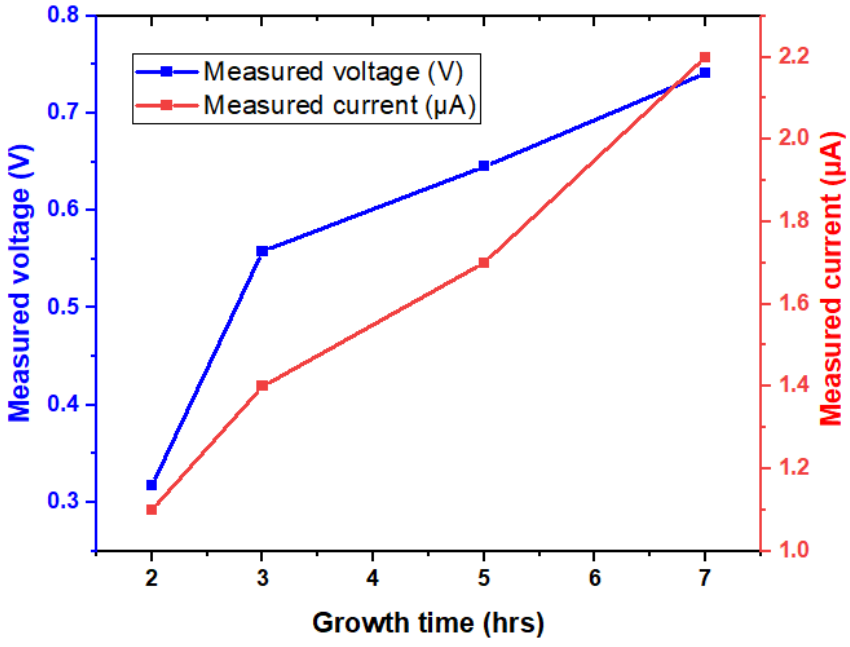

Fig. 5. I-V plot of measured voltage and current based on growth time

4. Conclusions

Due to the low cost and simple of manufacturing process, excellent efficiency, and environmental friendliness, DSSCs are the third generation of photovoltaic cells. The main goals of this review are the synthesis of ZnO nanorods on ITO and the characterization of the structural, optical, and electrical properties of the synthesized ZnO nanorods. The main focus is on the electrical characterization as the obtained I-V characteristics, maximum voltage and maximum current define the value of fully fabricated ZnO nanorods DSSC. Five layers including ITO glass, ZnO nanorods, ruthenizer, electrolyte and silver paste-coated ITO glass comprise a fully fabricated device. Ruthenium is deposited as a dye on a layer of ZnO nanorods. Four samples with different ZnO nanorods growth times are analysed to measure current and voltage under sunlight. Each sample has a surface area of 3 cm^2. A4 has the highest maximum voltage and current, resulting in 0.741 V and 2.2 A. Therefore, samples A4 exhibits the best voltage and current performance with ZnO nanorods growth time of 7 hrs thus showing that the growth time affects the morphology structure in terms of structural, optical and electrical properties of the ZnO nanorods photoanode in DSSC.

Acknowledgment

This research was funded by a grant from Ministry of Higher Education of Malaysia (FRGS Grant FRGS/1/2020/FTKEE-CETRI/F00454)

References

[1] Sharma, Shruti, Kamlesh Kumar Jain, and Ashutosh Sharma. 2015. “Solar Cells: In Research and Applications—A Review.” *Materials Sciences and Applications* 06 (12): 1145–55. https://doi.org/10.4236/msa.2015.612113

[2] Mertens, Konrad. *Photovoltaics: fundamentals, technology, and practice*. John Wiley & Sons, 2018.

[3] Chandiran, Aravind Kumar, Mojtaba Abdi-Jalebi, Mohammad K. Nazeeruddin, and Michael Grätzel. "Analysis of electron transfer properties of ZnO and TiO_2 photoanodes for dye-sensitized solar cells." *ACS nano* 8, no. 3 (2014): 2261-2268. https://doi.org/10.1021/nn405535j

[4] Shanmugam, Mariyappan, Braden Bills, Mahdi Farrokh Baroughi, and David Galipeau. "Electron transport in dye sensitized solar cells with TiO 2/ZnO core-shell photoelectrode." In *2010 35th IEEE Photovoltaic Specialists Conference*, pp. 003256-003259. IEEE, 2010. https://doi.org/10.1109/PVSC.2010.5616818

[5] Nizamuddin, Ahmad, Faiz Arith, Jia Rong, Muhammad Zaimi, A. Shamsul Rahimi, and Shahrizal Saat. "Investigation of copper (I) thiocyanate (CuSCN) as a hole transporting layer for perovskite solar cells application." *Journal of Advanced Research in Fluid Mechanics and Thermal Sciences* 78, no. 2 (2020): 153-159. https://doi.org/10.37934/arfmts.78.2.153159

[6] Dzikri, Istighfari, Michael Hariadi, Retno Wigajatri Purnamaningsih, and Nji Raden Poespawati. "Analysis of the role of hole transport layer materials to the performance of perovskite solar cell." In *E3S Web of Conferences*, vol. 67, p. 01021. EDP Sciences, 2018. https://doi.org/10.1051/e3sconf/20186701021

[7] O'Regan, Brian, Frank Lenzmann, Ruud Muis, and Jeannette Wienke. "A solid-state dye-sensitized solar cell fabricated with pressure-treated P25− TiO_2 and CuSCN: Analysis of pore filling and IV characteristics." *Chemistry of Materials* 14, no. 12 (2002): 5023-5029. https://doi.org/10.1021/cm020572d

[8] Sharma, Khushboo, Vinay Sharma, and S. S. Sharma. 2018. “Dye-Sensitized Solar Cells: Fundamentals and Current Status.” *Nanoscale Research Letters* 13.https://doi.org/10.1186/s11671-018-2760-6

[9] Waltz, William L. 1984. “The Study of Fast Processes and Transient Species by Electron Pulse Radiolysis.” *Radiation Physics and Chemistry (1977)* 23 (4): 491. https://doi.org/10.1016/0146-5724(84)90144-4

[10] Hagfeldt, Anders, and Michael Gratzel. 2000. “Hagfeldt, Grätzel - 2000 - Molecular Photovoltaics - Accounts of Chemical Research.Pdf - Unknown.Pdf - Unknown.Pdf.” *Accounts of Chemical Research* 33 (5): 269–77. https://doi.org/10.1021/ar980112j

[11] Ganesan, S., B. Muthuraaman, Vinod Mathew, J. Madhavan, P. Maruthamuthu, and S. Austin Suthanthiraraj. 2008. “Performance of a New Polymer Electrolyte Incorporated with Diphenylamine in Nanocrystalline Dye-Sensitized Solar Cell.” *Solar Energy Materials and Solar Cells* 92 (12): 1718–22. https://doi.org/10.1016/j.solmat.2008.08.004

[12] Ragoussi, Maria Eleni, Mine Ince, and Tomás Torres. 2013. “Recent Advances in Phthalocyanine-Based Sensitizers for Dye-Sensitized Solar Cells.” *European Journal of Organic Chemistry*, no. 29: 6475–89.

https://doi.org/10.1002/ejoc.201301009
[13] Zhang, Zhen, and John T. Yates. 2010. "Direct Observation of Surface-Mediated Electron-Hole Pair Recombination in TiO_2(110)." *Journal of Physical Chemistry C* 114 (7): 3098–3101. https://doi.org/10.1021/jp910404e
[14] Raghavan, Nivea, Sakthivel Thangavel, and Gunasekaran Venugopal. 2015. "Enhanced Photocatalytic Degradation of Methylene Blue by Reduced Graphene-Oxide/Titanium Dioxide/Zinc Oxide Ternary Nanocomposites." *Materials Science in Semiconductor Processing* 30: 321–29. https://doi.org/10.1016/j.mssp.2014.09.019
[15] Ni, Meng, Michael K.H. Leung, Dennis Y.C. Leung, and K. Sumathy. 2007. "A Review and Recent Developments in Photocatalytic Water-Splitting Using TiO_2 for Hydrogen Production." *Renewable and Sustainable Energy Reviews* 11 (3): 401–25. https://doi.org/10.1016/j.rser.2005.01.009
[16] Sahoo, D D, and G S Roy. 2013. "The Effects of Pt Doping on the Photo-Reactivity of TiO_2." *Researcher* 5 (1): 1–13.
[17] Nivea, R., V. Gunasekaran, R. Kannan, T. Sakthivel, and K. Govindan. 2014. "Enhanced Photocatalytic Efficacy of Hetropolyacid Pillared TiO_2 Nanocomposites." *Journal of Nanoscience and Nanotechnology* 14 (6): 4383–86. https://doi.org/10.1166/jnn.2014.8655
[18] Cheung, S. H., P. Nachimuthu, A. G. Joly, M. H. Engelhard, M. K. Bowman, and S. A. Chambers. 2007. "N Incorporation and Electronic Structure in N-Doped TiO_2(1 1 0) Rutile." *Surface Science* 601 (7): 1754–62. https://doi.org/10.1016/j.susc.2007.01.051
[19] Hagberg, Daniel P., Jun Ho Yum, Hyo Joong Lee, Filippo De Angelis, Tannia Marinado, Karl Martin Karlsson, Robin Humphry-Baker, et al. 2008. "Molecular Engineering of Organic Sensitizers for Dye-Sensitized Solar Cell Applications." *Journal of the American Chemical Society* 130 (19): 6259–66. https://doi.org/10.1021/ja800066y
[20] Zhang, Shufang, Xudong Yang, Youhei Numata, and Liyuan Han. 2013. "Highly Efficient Dye-Sensitized Solar Cells: Progress and Future Challenges." *Energy and Environmental Science* 6 (6): 1443–64. https://doi.org/10.1039/c3ee24453a
[21] Yella, Aswani, Hsuan Wei Lee, Hoi Nok Tsao, Chenyi Yi, Aravind Kumar Chandiran, Md Khaja Nazeeruddin, Eric Wei Guang Diau, Chen Yu Yeh, Shaik M. Zakeeruddin, and Michael Grätzel. 2011. "Porphyrin-Sensitized Solar Cells with Cobalt (II/III)-Based Redox Electrolyte Exceed 12 Percent Efficiency." *Science* 334 (6056): 629–34. https://doi.org/10.1126/science.1209688
[22] Noorasid, Nur Syamimi, Faiz Arith, Ahmad Nizamuddin Mustafa, Mohd Asyadi Azam, Syazwan Hanani Meriam Suhaimy, and Oras A. Al-Ani. 2021. "Effect of Low Temperature Annealing on Anatase TiO_2 Layer as Photoanode for Dye-Sensitized Solar Cell." *Przeglad Elektrotechniczny* 97 (10): 12–16. https://doi.org/10.15199/48.2021.10.03
[23] Noorasid, Nur Syamimi, Faiz Arith, Ahmad Nizamuddin Muhammad Mustafa, Syazwan Hanani Meriam Suhaimy, Ahmad Syahiman Mohd Shah, and Mohd Asyadi Azam Mohd Abid. 2021. "Numerical Analysis of Ultrathin TiO_2 Photoanode Layer of Dye Sensitized Solar Cell by Using SCAPS-1D." *Proceedings - 2021 IEEE Regional Symposium on Micro and Nanoelectronics, RSM 2021*, no. August: 96–99. https://doi.org/10.1109/RSM52397.2021.9511600
[24] Noorasid, Nur Syamimi, Faiz Arith, Ahmad Nizamuddin Mustafa, Puvaneswaran Chelvanathan, Mohammad Istiaque Hossain, Mohd Asyadi Azam, and Nowshad Amin. "Improved performance of lead-free Perovskite solar cell incorporated with TiO_2 ETL and CuI HTL using SCAPs." *Applied Physics A* 129, no. 2 (2023): 132. https://doi.org/10.1007/s00339-022-06356-5
[25] Alias, Nur Syafiqah Nadiah Mohd, Faiz Arith, Nur Syamimi Noorasid, Hafez Sarkawi, Ahmad Nizamuddin Muhammad Mustafa, Mohd Muzafar Ismail, and Mohd Khanapiah Nor. 2022. "Study the Effect of Nickel and Aluminium Doped ZnO Photoanode in DSSC." *Telkomnika (Telecommunication Computing Electronics and Control)* 20 (5): 1117–24. https://doi.org/10.12928/telkomnika.v20i5.23013
[26] Alias, N. S. N. M., F. Arith, A. N. M. Mustafa, M. M. Ismail, S. A. M. Chachuli, and A. S. M. Shah. "Compatibility of Al-doped ZnO electron transport layer with various HTLs and absorbers in perovskite solar cells." *Applied Optics* 61, no. 15 (2022): 4535-4542. https://doi.org/10.1364/AO.455550
[27] Noorasid, Nur Syamimi, Faiz Arith, Ain Yasmin Firhat, Ahmad Nizamuddin Mustafa, and Ahmad Syahiman Mohd Shah. "SCAPS Numerical Analysis of Solid-State Dye-Sensitized Solar Cell Utilizing Copper (I) Iodide as Hole Transport Layer." *Engineering Journal* 26, no. 2 (2022): 1-10. https://doi.org/10.4186/ej.2022.26.2.1
[28] Noorasid, N. S., F. Arith, A. N. Mustafa, M. A. Azam, S. Mahalingam, P. Chelvanathan, and N. Amin. 2022. "Current Advancement of Flexible Dye Sensitized Solar Cell: A Review." *Optik* 254 (March): 168089. https://doi.org/10.1016/j.ijleo.2021.168089
[29] Carella, Antonio, Fabio Borbone, and Roberto Centore. 2018. "Research Progress on Photosensitizers for DSSC." *Frontiers in Chemistry* 6 (SEP): 1–24. https://doi.org/10.3389/fchem.2018.00481
[30] Sokolský, Michal, and Július Cirák. 2010. "Dye-Sensitized Solar Cells: Materials and Processes." *Acta Electrotechnica et Informatica* 10 (3): 78–81.
[31] Zagorac, Dejan, Christian Schön, Jelena Zagorac, Ilya Pentin Vladimirovich, and Martin Jansen. 2013. "Zinc Oxide: Connecting Theory and Experiment." *Processing and Application of Ceramics* 7 (3): 111–16. https://doi.org/10.2298/PAC1303111Z

[32] Kolodziejczak-Radzimska, Agnieszka, and Teofil Jesionowski. 2014. "Zinc Oxide-from Synthesis to Application: A Review." *Materials* 7 (4): 2833–81. https://doi.org/10.3390/ma7042833

[33] Yi, Gyu Chul, Chunrui Wang, and Won Il Park. 2005. "ZnO Nanorods: Synthesis, Characterization and Applications." *Semiconductor Science and Technology* 20 (4). https://doi.org/10.1088/0268-1242/20/4/003

[34] Polsongkram, D., P. Chamninok, S. Pukird, L. Chow, O. Lupan, G. Chai, H. Khallaf, S. Park, and A. Schulte. 2008. "Effect of Synthesis Conditions on the Growth of ZnO Nanorods via Hydrothermal Method." *Physica B: Condensed Matter* 403 (19–20): 3713–17. https://doi.org/10.1016/j.physb.2008.06.020

[35] Nishizawa, Hitoshi, Takuhiro Tani, and Kiyoshi Matsuoka. 1984. "Crystal Growth of ZnO by Hydrothermal Decomposition of Zn-EDTA." *Journal of the American Ceramic Society* 67 (6): C-98-C-100. https://doi.org/10.1111/j.1151-2916.1984.tb19720.x

[36] Baxter, Jason B., and Eray S. Aydil. 2005. "Nanowire-Based Dye-Sensitized Solar Cells." *Applied Physics Letters* 86 (5): 1–3https://doi.org/10.1063/1.1861510

[37] Mustaffa, Mohammad Aiman, Faiz Arith, Nur Syamimi Noorasid, Mohd Shahril Izuan Mohd Zin, Kok Swee Leong, Fara Ashikin Ali, Ahmad Nizamuddin Muhammad Mustafa, and Mohd Muzafar Ismail. 2022. "Towards a Highly Efficient ZnO Based Nanogenerator" *Micromachines* 13, no. 12: 2200. https://doi.org/10.3390/mi13122200

[38] Li, Xin, Chaoyang Li, Shengwen Hou, Akimitsu Hatta, Jinhong Yu, and Nan Jiang. 2015. "Thickness of ITO Thin Film Influences on Fabricating ZnO Nanorods Applying for Dye-Sensitized Solar Cell." *Composites Part B: Engineering* 74: 147–52. https://doi.org/10.1016/j.compositesb.2015.01.017

[39] Richhariya, Geetam, Anil Kumar, Perapong Tekasakul, and Bhupendra Gupta. 2017. "Natural Dyes for Dye Sensitized Solar Cell: A Review." *Renewable and Sustainable Energy Reviews* 69 (November 2016): 705–18. https://doi.org/10.1016/j.rser.2016.11.198